

Radiographic and computed tomographic assessment of the development of the antebrachia and elbow joints in Labrador Retrievers with and without medial coronoid disease

S. F. Lau^{1,3}; H. A. W. Hazewinkel²; G. Voorhout¹

¹Division of Diagnostic Imaging, Faculty of Veterinary Medicine, Utrecht University, Utrecht, The Netherlands;

²Department of Clinical Sciences of Companion Animals, Faculty of Veterinary Medicine, Utrecht University, Utrecht,

The Netherlands; ³Department of Veterinary Clinical Studies, Faculty of Veterinary Medicine, Universiti Putra Malaysia, Serdang, Malaysia

Keywords

Elbow joint, Labrador Retriever, medial coronoid disease, development

Summary

Objectives: To compare the development, monitored by radiography and computed tomography, of the antebrachia and elbow joints in seven Labrador Retrievers with healthy elbow joints and in seven Labrador Retrievers that developed medial coronoid disease (MCD), in order to determine whether disturbances in the development of the antebrachia and elbow joints, between the age of six and 17 weeks may lead to medial coronoid disease.

Methods: A prospective study of 14 Labrador Retrievers in their active growth stage was performed. The development of the antebrachia and elbow joints was assessed between six and 17 weeks of age using

radiography and computed tomography determining the development of secondary ossification centres, radioulnar length ratio, radial angulation, and inter-relationship between the humerus, ulna and radius.

Results: For the parameters of ossification of secondary ossification centres, radioulnar length ratio, radial angulation, and joint congruence evaluation, there was no significant difference in the development of the antebrachia and elbow joints of seven Labrador Retrievers positive and seven Labrador Retrievers negative for MCD at the age of six to 17 weeks.

Clinical significance: These findings demonstrate that the development of MCD in the Labrador Retrievers in our study was not related to any disturbance in the development of the antebrachia and elbow joints during the rapid growth phase.

Introduction

Medial coronoid disease, which includes fissuring and fragmentation of the medial coronoid process, and pathological lesions of cartilage and of subchondral bone of the medial coronoid process has been introduced as being a more representative term than fragmented medial coronoid process (1, 2). Despite the high incidence of medial coronoid disease in Labrador Retrievers and other breeds, the aetiopathogenesis of the disease has yet to be elucidated (2–4). Different theories have been postulated regarding the aetiopathogenesis of medial coronoid disease.

Current postulated factors contributing to medial coronoid disease include osteochondrosis, fatigue-induced microdamage of subchondral bone, different distribution of loading or forces within the joint such as tensile forces originating from the annular ligament, and shear stress between the contact area of the proximal radial head and axial border of the medial coronoid process during pronation and supination (5–8). Mechanical overloading of the ulnar surface due to joint incongruity with a shortened radius or under-development of the ulnar trochlear notch has also been suggested to cause or contribute to the disease (9, 10).

The postnatal development of the canine radius, ulna, and humerus has been investigated in small and large breed dogs, but there is a lack of information regarding the postnatal development of the radius, ulna, and humerus in the Labrador Retriever, a

Correspondence to:

Seng Fong Lau, DVM, PhD
Department of Veterinary Clinical Studies
Faculty of Veterinary Medicine
Universiti Putra Malaysia
43400 Serdang
Malaysia
Phone: +60 386 093 927
E-mail: lausengfong@hotmail.com

Vet Comp Orthop Traumatol 2015; 28: 186–192

<http://dx.doi.org/10.3415/VCOT-14-09-0144>

Received: September 21, 2014

Accepted: March 2, 2015

Epub ahead of print: March 25, 2015

breed with a high incidence of medial coronoid disease (2, 3, 11–20). Any disturbance of endochondral ossification may lead to abnormal skeletal development and maturation (20, 21). Abnormalities in the development and maturation of the elbow joint may occur in the first three to four months of life during the rapid growth phase. Hence, the aim of the present study was to compare the development, monitored by radiography and CT, of the antebrachium and elbow joint in dogs with healthy elbow joints and in dogs that developed medial coronoid disease, in order to determine whether disturbances in the development of the antebrachium and elbow joint between the age six and 17 weeks may contribute to the occurrence of medial coronoid disease.

Materials and methods

Data collection

This study was approved by the Ethics Committee of Utrecht University as required by Dutch legislation (D.E.C. 2009.III.06.050). Fourteen purpose-bred Labrador Retriever puppies (nine males, five females), originating from two litters of a medial coronoid disease positive dam and two medial coronoid disease positive sires, were monitored at two week intervals by radiography and computed tomography (CT) of the antebrachia and elbow joints, from six ($n = 7$) or seven ($n = 7$) weeks of age until euthanasia at the age of 15 weeks (2 dogs) or 17 weeks for another micro CT, necropsy and histological study (remaining 12 dogs) (11–12). The dogs were raised on a diet of commercial dog food and housed in groups of two or three dogs.

Radiographs of the elbow joints were made with a direct digital radiography system^a using 50 kVp and 8 mA. Only mediolateral and craniocaudal views of the elbow joints were obtained when the dogs were between six and 11 weeks of age. Craniolateral-caudomedial oblique and extended supinated mediolateral views were included from 12 weeks onward (11). For CT, the dogs were anaesthetized and positioned in dorsal recumbency on the CT

scanning table with the elbow joints extended about 135°. The antebrachia were positioned parallel to each other and as symmetrically as possible at the same level using a custom-made positioning device. Transverse views were made with a third-generation single-slice helical CT scanner^b using 120 kVp and 120 mA with an exposure time of 1 second, and a pitch of 1.0. One millimetre thick slices of the elbow joints were made with the joints in neutral position as described previously (11).

The results of radiography, CT, micro CT, necropsy and histological examination of the elbow joints of these dogs have been described previously (11, 12). Of the 14 dogs, seven (four males, three females) were medial coronoid disease-negative and six (five males, one female) were bilaterally medial coronoid disease-positive. One female dog was medial coronoid disease-positive unilaterally.

From the series of radiographs and CT images from six until 17 weeks of age, including two dogs which were euthanized at the age of 15 weeks, the development of the antebrachia and elbow joints was assessed on the basis of the development of secondary ossification centres, the growth in length of the radius and ulna, radial angulation, and the inter-relationship between the humerus, ulna and radius. All assessments and measurements were performed by a single observer (SFL) who was unaware of the medial coronoid process status of the dogs at the time of the measurements.

Secondary ossification centres

From the lateral radiographs of the antebrachii, the development of the olecranal apophysis, medial humeral epicondyle, and ulnar styloid process was assessed and classified according to the stage of ossification and the shape (irregular ossification, round, rounded edges, proper anatomical shape) (16, 20). Ossification of the anconeal process was assessed on serial CT images, and the stage of ossification was classified according to the shape and delineation (no evidence of

ossification, irregular ossification, and proper anatomical shape).

Radioulnar length ratio

The radioulnar length ratio was calculated using measurements from the serial mediolateral radiographic projections. The diaphyseal length of the radius was measured from the mid-point of the proximal radial growth plate to the mid-point of the distal radial growth plate along a straight line. The ulnar diaphyseal length was measured from the most proximal part of the proximal ulnar metaphysis to the most distal part of the distal ulnar metaphysis along a straight line. The radioulnar length ratio was calculated by dividing the length of the radius by the length of the ulna.

Centre of rotation of angulation methodology

For radial alignment quantification, the centre of rotation of angulation (CORA) method was used (22). On the craniocaudal radiographic projection, joint orientation lines were drawn along the proximolateral aspect and the proximomedial aspect of the radial head and, at the carpal joint level, along the distolateral aspect and the distomedial aspect of the distal radius (►Figure 1a). The medial proximal radial angle and lateral distal radial angle were determined from the craniocaudal radiograph (►Figure 1b) (22). Sagittal radial orientation was assessed on the mediolateral radiographic projection, with joint orientation lines drawn along the proximo-cranial and proximo-caudal aspect of the radial head and, at the carpal joint level, along the disto-cranial and disto-caudal aspect of the radius (►Figure 1c). Joint orientation angles in the mediolateral radiographic projection, namely, the proximal cranial radial angle and distal caudal radial angle, were determined as described previously (►Figure 1d) (22). The radial procurvatum angle was measured at the point at which the two separate straight mid-diaphyseal lines intersected (►Figure 1d).

Joint congruence evaluation

Radioulnar congruity was assessed from CT images as described before and

a Philips Digital Rad TH: Philips, Eindhoven, The Netherlands

b Philips Secura: Philips, Eindhoven, The Netherlands

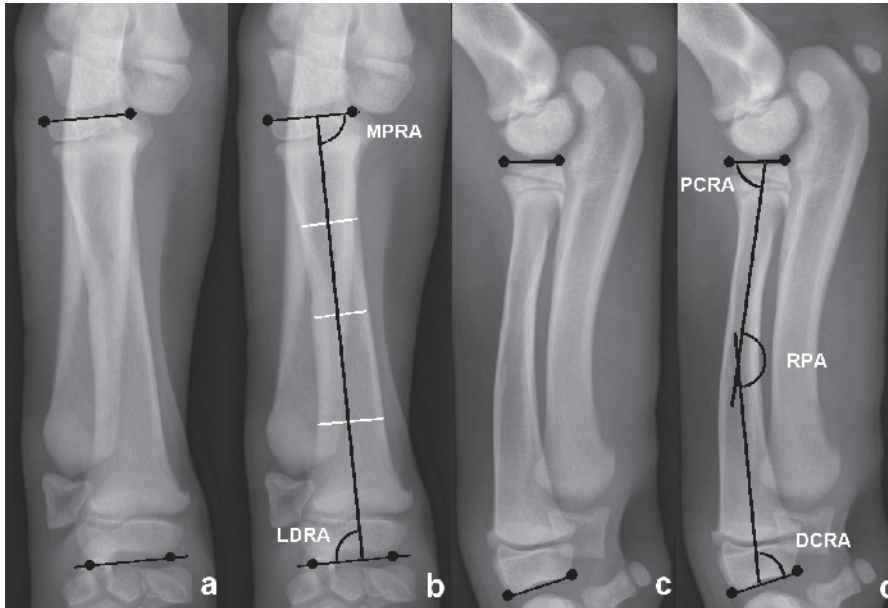


Figure 1 Right antebrachium of a normal dog at nine weeks of age. **a, b**) Craniocaudal radiographs: 'joint orientation lines' connect two points (circles) at the medial and lateral extent of the proximal and distal radius, respectively. The radial anatomic axis was drawn by connecting the mid-diaphyseal points along the length of the radius. **b**) Medial proximal radial angle (MPRA) and lateral distal radial angle (LDRA): the angles of the anatomic axis with both joint orientation lines. **c, d**) Mediolateral radiographs: joint orientation lines were drawn across the two points (circles) at the cranial and caudal extent of the proximal and distal radius, respectively. The radial anatomic axes were determined by connecting two mid-diaphyseal lines each for the proximal half and the distal half of the radial segments. The proximal cranial radial angle (PCRA) and distal caudal radial angle (DCRA) were determined by measuring the angles from intersecting anatomic axes and joint reference lines. The radial procurvatum angle (RPA) was determined from the intersecting point of the two separate straight mid-diaphyseal lines.

measured three times on the reconstructed sagittal and dorsal CT images obtained from 12 or 13 weeks until 15 weeks in the two dogs that were euthanatized at that age, and until 16 or 17 weeks of age in the remaining dogs (23). Sagittal plane reconstructions were made at the base of medial coronoid process at the junction

with the trochlear notch (► Figure 2a); a circle was drawn along the ulnar trochlear notch (► Figure 2b). Radioulnar joints were considered congruent when there was no step between the most proximal epiphyseal borders of the radius and the circle. In reconstructed images in the dorsal plane at both the middle and the apex

of the medial coronoid process (► Figure 2a), the distance between the most proximal ulnar surface and the most proximomedial aspect of radial head was measured (► Figure 2c and d). Humeroulnar joint congruence was assessed on a series of sagittal plane reconstructions and the joint was considered congruent when there was no evidence of mismatch in between the curvature of the trochlear notch and humeral trochlea. Humeroulnar joint congruence was classified as present or absent.

Statistical analysis

Statistical analyses were performed using a statistical software package^c. The non-parametric Kruskal-Willis test was used to analyse the data of the secondary ossification centres study because the dependent outcome was an ordinal score; differences were considered statistically significant at $p < 0.05$. Linear mixed models containing both fixed and random effects were used to analyse the radioulnar length ratio, medial proximal radial angle, lateral distal radial angle, proximal cranial radial angle, distal caudal radial angle, radial procurvatum angle, and radioulnar joint congruence evaluation. Model selection was based on the Akaike Information Criterion. Conditions for the use of mixed models, including the normal distribution of the data, were assessed by analysing the residuals (PP and QQ plots) of the acquired models; no violations of these conditions were observed. Data are expressed as mean \pm SD (► Table 1,

^c SPSS Version 20.0: SPSS Inc., Chicago, IL, USA

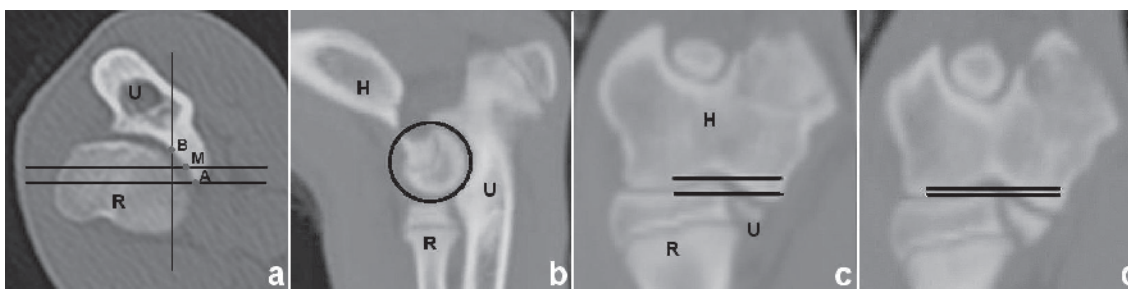


Figure 2 Computed tomographic images obtained from the right elbow joint of a dog at 17 weeks of age. **a**) Transverse computed tomographic slice demonstrates the orientation of reformatted images. The sagittal plane was reconstructed at the region of the base (B) of the medial coronoid process. Two dorsal planes were reconstructed at the mid (M), and apex (A) of the medial

coronoid process. **b**) In the sagittal plane, a circle was drawn along the ulnar trochlear notch to detect the step defect in the radioulnar joint. Dorsal planes reconstructed at the A (**c**) and M (**d**) of the medial coronoid process with the distance measured in between the most proximal ulnar surface with the most proximomedial aspect of the radial head. U = ulna; R = radius; H = humerus.

Table 1 Measurements used to investigate the development of the antebrachia and elbow joints at different ages (in weeks).

	Age in weeks					
	6–7	8–9	10–11	12–13	14–15	16–17
Radioulnar length ratio						
RU (ratio)	0.778 ± 0.01	0.784 ± 0.01	0.783 ± 0.01	0.784 ± 0.01	0.788 ± 0.01	0.791 ± 0.01
Centre of rotation of angulation methodology						
MPRA (°)	89.3 ± 2.5	89.9 ± 2.2	92.4 ± 2.7	92.9 ± 2.2	92.7 ± 2.0	94.8 ± 2.3
LDRA (°)	83.8 ± 3.0	85.4 ± 2.3	89.5 ± 2.1	86.0 ± 2.2	86.9 ± 2.2	87.9 ± 2.0
PCRA (°)	85.2 ± 2.2	84.5 ± 2.0	87.4 ± 2.2	89.4 ± 1.5	90.1 ± 1.8	89.0 ± 2.3
DCRA (°)	78.7 ± 3.1	75.9 ± 2.8	78.4 ± 2.5	81.1 ± 2.8	78.8 ± 2.7	76.5 ± 2.7
RPA (°)	168.3 ± 0.4	168.4 ± 0.5	168.3 ± 0.3	168.3 ± 0.4	168.4 ± 0.5	168.2 ± 0.4
Radioulnar congruence						
Apex (mm)	-	-	-	1.58 ± 0.18	1.52 ± 0.17	1.53 ± 0.18
Mid (mm)	-	-	-	0.86 ± 0.02	0.87 ± 0.02	0.86 ± 0.02

Values are shown as mean ± SD. RU = radioulnar; MPRA = medial proximal radial angle; LDRA = lateral distal radial angle; PCRA = proximal cranial radial angle; DCRA = distal caudal radial angle; RPA = radial procurvatum angle.

►Table 2), and differences were considered statistically significant at $p < 0.05$.

Results

Secondary ossification centres

The olecranal apophysis was not yet ossified in nine dogs, but it was visible as an ill-defined area of ossification in five dogs at six or seven weeks of age. It was detectable in all dogs at eight or nine weeks of age. The structure was well-delineated with rounded edges at 10 or 11 weeks of age in all dogs. The olecranal apophysis attained its proper anatomical shape at 14 or 15 weeks of age. With regard to ossification of the medial humeral epicondyle, the secondary ossification centres were either ill-defined areas of ossification (six dogs) or round (eight dogs) at six or seven weeks of age. In all dogs, the medial humeral epicondyle attained its rounded edges by 10 or 11 weeks of age and acquired its proper anatomical shape in the subsequent weeks.

At six or seven weeks of age, the appearance of the ulnar styloid process was either an irregular area of ossification (eight dogs) or had a rectangular shape with the width larger than the height (six dogs). Thereafter, the ulnar styloid process ossified gradually into a cone shape with irregular ossification at its apex by 14 or 15 weeks of age. The

apex of the ulnar styloid process was well-defined and delineated at 16 or 17 weeks of age (►Figure 3). The earliest age at which a small area of irregular ossification in the region of the anconeal process could be detected was 11 weeks, and this area of ossification was connected with the rest of the ulna (►Figure 4b). None of the dogs had evidence of a separate ossification centre in the anconeal process, and by 15 or 16 weeks of age, all anconeal processes had attained

their proper anatomic shape (►Figure 4c). Statistically, the ossification of secondary ossification centre did not differ significantly between medial coronoid disease positive and medial coronoid disease negative status ($p = 0.66–0.82$).

Radioulnar length ratio

The mean (± SD) radioulnar length ratio for the canine antebrachia is shown in

Table 2

Measurements used to investigate the development of the antebrachia and elbow joints of dogs with a different medial coronoid process status.

	Medial coronoid process status	
	MCD negative	MCD positive
Radioulnar length ratio		
RU (ratio)	0.786 ± 0.01	0.783 ± 0.01
Centre of rotation of angulation methodology		
MPRA (°)	91.2 ± 2.2	92.3 ± 2.5
LDRA (°)	87.5 ± 2.3	87.3 ± 2.4
PCRA (°)	88.6 ± 2.0	85.7 ± 2.0
DCRA (°)	77.7 ± 2.9	78.2 ± 2.7
RPA (°)	168.3 ± 0.4	168.4 ± 0.4
Radioulnar congruence evaluation		
Apex (mm)	1.54 ± 0.16	1.51 ± 0.13
Mid (mm)	0.86 ± 0.02	0.86 ± 0.02

Values are shown as mean ± SD. MCD = medial coronoid disease; RU = radio-ulnar; MPRA = medial proximal radial angle; LDRA = lateral distal radial angle; PCRA = proximal cranial radial angle; DCRA = distal caudal radial angle; RPA = radial procurvatum angle.

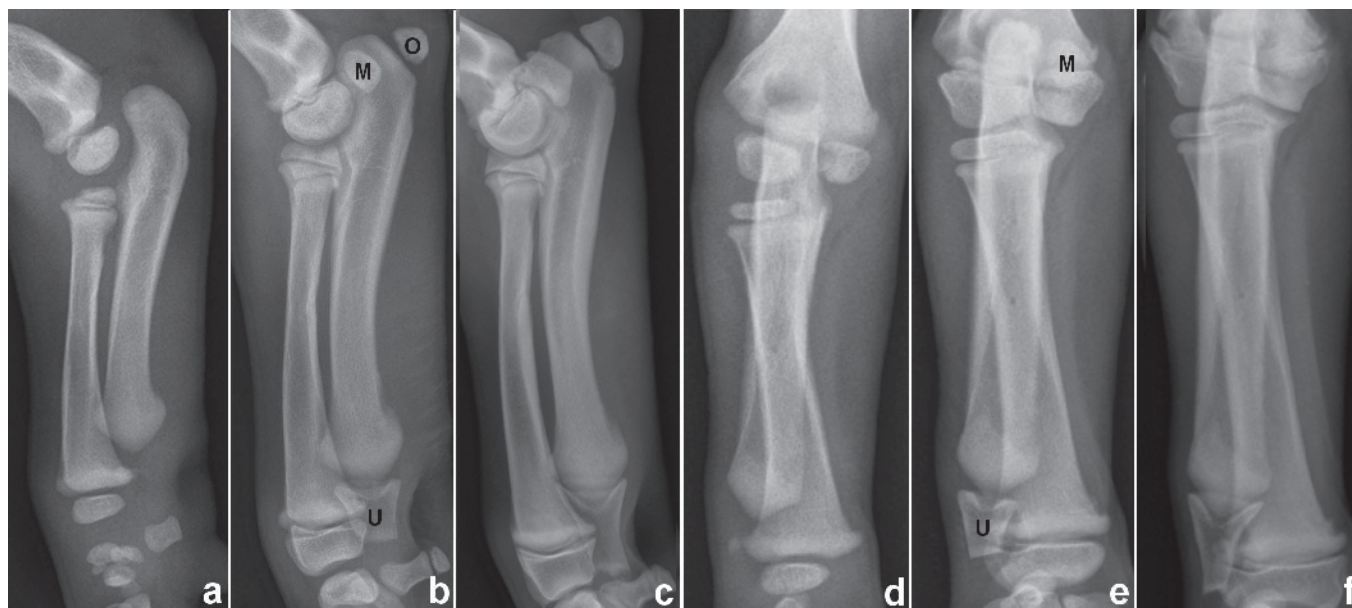


Figure 3 Radiographic images of the right antebrachium of the same Labrador Retriever diagnosed negative for medial coronoid disease taken at different ages. **a)** Mediolateral view taken at the age of six weeks; absence of the olecranal apophysis, ill-defined secondary ossification centre of the medial humeral epicondyle, and irregular secondary ossification centre of the ulnar styloid process can be observed. **b)** Mediolateral view taken at the age of 10 weeks; well-delineated and rounded olecranal apophysis and medial humeral epicon-

dyle, and a rectangular shaped ulnar styloid process (width equal to height) can be observed. **c)** Mediolateral view taken at the age of 14 weeks; all the secondary ossification centres had reached their proper anatomical shape, but were not yet fused with the diaphysis. Irregular ossification can still be observed at the apex of the ulnar styloid process. Craniocaudal view of the same dog taken at **(d)** six weeks, **(e)** 10 weeks, and **(f)** 14 weeks of age. O = olecranal apophysis; M = medial humeral epicondyle; U = ulnar styloid process.

► Table 1 and ► Table 2. The radioulnar length ratio increased significantly with age ($p < 0.001$) but was not affected by medial coronoid process status ($p = 0.06$).

Centre of rotation of angulation methodology

The medial proximal radial angle, lateral distal radial angle, proximal cranial radial angle, distal caudal radial angle, and pro-

curvatum angle are shown in ► Table 1 and ► Table 2, by age and medial coronoid process status. Medial proximal radial angle and lateral distal radial angle increased with age ($p \leq 0.001$), whereas proximal cranial radial angle ($p = 0.14$), distal caudal radial angle ($p = 0.28$) and radial procurvatum angle ($p = 0.58$) did not (► Table 1). Medial proximal radial angle, lateral distal radial angle, proximal cranial radial angle, distal caudal radial angle, and radial pro-

curvatum angle were not significantly different in medial coronoid disease positive and medial coronoid disease negative dogs ($p = 0.17$ – 0.67) (► Table 2).

Joint congruence evaluation

In the neutral position, radioulnar and humeroulnar incongruency were not detected from 12 or 13 weeks until 15 weeks in the two dogs that were euthanized at that age, and until 16 or 17 weeks of age in the remaining dogs. No step defect was observed on CT images. The mean \pm SD distance between the most proximal ulnar surface and the most proximomedial aspect of radial head is given in ► Table 1 and ► Table 2. The distance was not affected significantly by age ($p = 0.22$ – 0.67) or medial coronoid disease positive or negative status ($p = 0.57$ – 0.89).

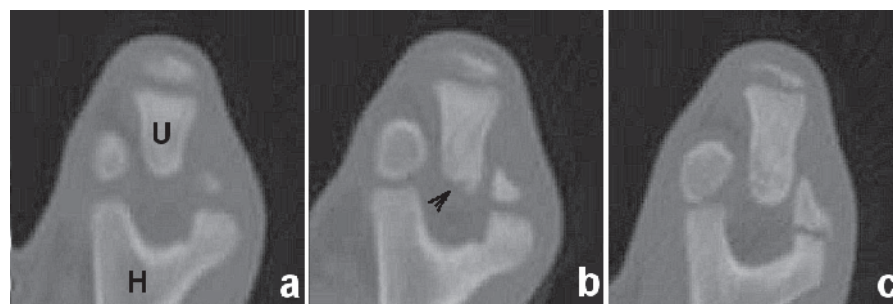


Figure 4 Transverse slice of the computed tomographic images of the left elbow obtained from dogs at different ages showing the ossification of the anconeal process. At **a)** 10 weeks of age with absence of the ossification of the anconeal process, **(b)** 12 weeks of age with an incomplete ossified anconeal process without a separation line with the ulnar diaphysis (arrow), and **(c)** 14 weeks of age with a proper anatomical shape of the anconeal process. U = ulnar; H = humerus.

Discussion

There were no significant differences found in the development of the antebrachia and

elbow joints of dogs that were positive or negative for medial coronoid disease between the ages of six to 17 weeks for the parameters examined (ossification of secondary ossification centres, radioulnar length ratio, medial proximal radial angle, lateral distal radial angle, proximal cranial radial angle, distal caudal radial angle, radial procurvatum angle, and joint congruence evaluation). It is crucial to investigate the development of the elbow joints at a very young age since medial coronoid disease can occur as early as 14 weeks of age, even though some investigators consider that radiographic findings regarding the structural anatomy of the bones are not accurate before 16 weeks of age due to incomplete ossification (11, 12, 17, 19). Our previous studies proved that CT was more sensitive (30.8%) than radiography (0%) in detecting early medial coronoid disease, with the earliest signs detectable at 14 weeks of age (11, 12).

Although there was some variation in the development of the secondary ossification centres among the 14 pairs of elbow joints studied, the proper anatomical shape was attained in all elbows by 16 or 17 weeks of age. Secondary ossification centres of the olecranal apophysis, medial humeral epicondyle, and ulnar styloid process were not fully fused with the diaphysis at the age of 16 or 17 weeks. The ossification of the anconeal process in Labrador Retrievers differs from that in some other breeds (16, 20, 24). Unlike Great Danes, for instance Labrador Retrievers do not have a clearly distinguishable, separate secondary ossification centre in the anconeal process. Ossification started from the base and was completed within two weeks.

Although none of the measurements obtained using CORA were significantly different between medial coronoid disease positive and medial coronoid disease negative dogs, we have provided breed specific joint reference angles from images of growing Labrador Retrievers. This might be useful in the planning of deformity correction in future cases. These joint reference angles can be used as well in the identification of the location and magnitude of a deformity case.

Radioulnar and humeroulnar joint congruence evaluation were not different in

dogs with and without medial coronoid disease. We evaluated the joint congruence from the age of 12–13 weeks onward because the large joint space before the age of 12 weeks made measurements inaccurate. Bones had almost achieved their proper anatomic shape by 12 weeks even though they were still undergoing remodelling. We conclude that joint incongruity does not play a role in the development of medial coronoid disease in Labrador Retrievers in our study. This was further supported by the later necropsy examination where no evidence of radioulnar and humeroulnar incongruity was found in medial coronoid disease-positive limbs (11, 12).

All measurements should be interpreted with caution because the cartilage layers are not visible on radiographic and CT images. Although a CT image is used as a gold standard to detect radioulnar incongruency, mild radioulnar incongruency may be missed on CT due to partial volume effects (25). Furthermore, we cannot rule out the dynamic radioulnar longitudinal incongruency as proposed by using static radiography (26).

We monitored the growth of Labrador Retrievers during a period of rapid growth, and without the evidence of signs of secondary degenerative joint changes, such as subtrochlear sclerosis and periarticular osteophytosis. Therefore we are confident that these medial coronoid disease positive elbows do represent the incipient medial coronoid disease. Absence of periarticular osteophytosis in all images enabled us to identify the bone edges and landmarks accurately.

Conclusions

On the basis of our findings, we conclude that the development of the medial coronoid disease in Labrador Retrievers in our study was not related to any disturbance in the development of the antebrachia and elbow joints during the rapid growth phase. Further breed specific studies would be necessary to determine whether such disturbances play a role in the aetiopathogenesis of medial coronoid disease in other breeds.

Conflict of interest

None declared.

References

1. Moores AP, Benigni L, Lamb CR. Computed tomography versus arthroscopy for detection of canine elbow dysplasia lesions. *Vet Surg* 2008; 37: 390–398.
2. Fitzpatrick N, Smith TJ, Evans RB, et al. Radiographic and arthroscopic findings in the elbow joints of 263 dogs with medial coronoid disease. *Vet Surg* 2009; 38: 213–223.
3. Meyer-Lindenberg A, Langhann A, Fehr M, et al. Prevalence of fragmented medial coronoid process of the ulna in lame adult dogs. *Vet Rec* 2002; 151: 230–234.
4. Seyrek-Intas D, Michele U, Tacke S, et al. Accuracy of ultrasonography in detecting fragmentation of the medial coronoid process in dogs. *J Am Vet Med Assoc* 2009; 234: 480–485.
5. Olsson SE. Lameness in the dog: A review of lesions causing osteoarthritis of the shoulder, elbow, hip, stifle and hock joints. *J Am Anim Hosp Assoc* 1975; 1: 363.
6. Danielson KC, Fitzpatrick N, Muir P, et al. Histomorphometry of fragmented medial coronoid process in dogs: a comparison of affected and normal coronoid processes. *Vet Surg* 2006; 35: 501–509.
7. Wolschrijn CF, Weijts WA. Development of the trabecular structure within the ulnar medial coronoid process of young dogs. *Anat Rec A Discov Mol Cell Evol Biol* 2004; 278: 514–519.
8. Hulse D, Young B, Beale B, et al. Relationship of the biceps-brachialis complex to the medial coronoid process of the canine ulna. *Vet Comp Orthop Traumatol* 2010; 23: 173–176.
9. Preston CA, Schulz KS, Taylor KT, et al. In vitro experimental study of the effect of radial shortening and ulnar ostectomy on contact patterns in the elbow joint of dogs. *Am J Vet Res* 2001; 62: 1548–1556.
10. Wind A. Elbow incongruity and developmental elbow diseases in the dog: Part I. *J Am Anim Hosp Assoc* 1986; 22: 711–724.
11. Lau SF, Wolschrijn CF, Hazewinkel HAW, et al. The early development of medial coronoid disease (MCD) in growing Labrador Retrievers: Radiographic, computed tomographic, necropsy and micro-computed tomographic findings. *Vet J* 2013; 197: 724–730.
12. Lau SF, Hazewinkel HAW, Grinwis GCM, et al. Delayed endochondral ossification in early medial coronoid disease (MCD): A morphological and immunohistochemical evaluation in growing Labrador retrievers. *Vet J* 2013; 197: 731–738.
13. Hare WC. The ages at which the centers of ossification appear roentgenographically in the limb bones of the dog. *Am J Vet Res* 1961; 22: 825–835.
14. Fox SM, Bloomberg MS, Bright RM. Developmental anomalies of the canine elbow. *J Am Anim Hosp Assoc* 1983; 19: 605–615.
15. Guthrie S, Plummer JM, Vaughan LC. Post natal development of the canine elbow joint: A light and electron microscopical study. *Res Vet Sci* 1992; 52: 67–71.

16. Voorhout G, Nap RC, Hazewinkel HAW. A radiographic study on the development of the antebrachium in Great Dane pups, raised under standardized conditions. *Vet Radiol Ultrasound* 1994; 35: 271–276.
17. Breit S, Künzel W, Seiler S. Variation in the ossification process of the anconeal and medial coronoid processes of the canine ulna. *Res Vet Sci* 2004; 77: 9–16.
18. Sereda CW, Lewis DD, Radasch RM, et al. Descriptive report of antebrachial growth deformity correction in 17 dogs from 1999 to 2007, using hybrid linear-circular external fixator constructs. *Can Vet J* 2009; 50: 723–732.
19. Wind AP, Packard ME. Elbow incongruity and developmental elbow diseases in the dog: Part II. *J Am Anim Hosp Assoc* 1986; 22: 725–730.
20. Voorhout G, Hazewinkel HAW. A radiographic study on the development of the antebrachium in Great Dane pups on different calcium intakes. *Vet Radiol* 1987; 28: 152–157.
21. Mackie E, Ahmed Y, Tatarczuch L, et al. Endochondral ossification: How cartilage is converted into bone in the developing skeleton. *Int J Biochem Cell Biol* 2008; 40: 46–62.
22. Fox DB, Tomlinson JL, Cook JL, et al. Principles of uniapical and biapical radial deformity correction using dome osteotomies and the center of rotation of angulation methodology in dogs. *Vet Surg* 2006; 35: 67–77.
23. Kramer A, Holsworth IG, Wisner ER, et al. Computed tomographic evaluation of canine radioulnar incongruence in vivo. *Vet Surg* 2006; 35: 24–29.
24. Frazho JK, Graham J, Peck JN, et al. Radiographic evaluation of the anconeal process in skeletally immature dogs. *Vet Surg* 2010; 39: 829–832.
25. De Rycke LM, Gielen IM, van Bree H, et al. Computed tomography of the elbow joint in clinically normal dogs. *Am J Vet Res* 2002; 63: 1400–1407.
26. Fitzpatrick N, Yeadon R. Working algorithm for treatment decision making for developmental disease of the medial compartment of the elbow in dogs. *Vet Surg* 2009; 38: 285–300.

